Characterization of nascent HDL particles and microparticles formed by ABCA1-mediated efflux of cellular lipids to apoA-I

Phu T. Duong, Heidi L. Collins, Margaret Nickel, Sissel Lund-Katz, George H. Rothblat, and Michael C. Phillips[1]

Division of GI/Nutrition, Children's Hospital of Philadelphia, University of Pennsylvania School of Medicine, Philadelphia, PA 19104-4318

Abstract The nascent HDL created by ABCA1-mediated efflux of cellular phospholipid (PL) and free (unesterified) cholesterol (FC) to apolipoprotein A-I (apoA-I) has not been defined. To address this issue, we characterized the lipid particles released when J774 mouse macrophages and human skin fibroblasts in which ABCA1 is activated are incubated with human apoA-I. In both cases, three types of nascent HDL containing two, three, or four molecules of apoA-I per particle are formed. With J774 cells, the predominant species have hydrodynamic diameters of ~9 and 12 nm. These discoidal HDL particles have different FC contents and PL compositions, and the presence of acidic PL causes them to exhibit α-electrophoretic mobility. These results are consistent with ABCA1 located in more than one membrane microenvironment being responsible for the production of the heterogeneous HDL. Activation of ABCA1 also leads to the release of apoA-I-free plasma membrane vesicles (microparticles). These larger, spherical particles released from J774 cells have the same PL composition as the 12 nm HDL and contain CD14 and ganglioside, consistent with their origin being plasma membrane raft domains. The various HDL particles and microparticles are created concurrently, and there is no precursor-product relationship between them. Importantly, a large fraction of the cellular FC effluxed from these cells by ABCA1 is located in microparticles. Collectively, these results show that the products of the apoA-I/ABCA1 interaction include discoidal HDL particles containing different numbers of apoA-I molecules. The cellular PLs and cholesterol incorporated into these nascent HDL particles originate from different cell membrane domains.—Duong P. T., H. L. Collins, M. Nickel, S. Lund-Katz, G. H. Rothblat, and M. C. Phillips. **Characterization of nascent HDL particles and microparticles formed by ABCA1-mediated efflux of cellular lipids to apoA-I.** *J. Lipid Res.* 2006. **47:** 832–843.

HDL functions as an acceptor lipoprotein in the process of reverse cholesterol transport from peripheral tissues (1–3), including the transport of cholesterol away from cells in the vessel wall (and from foam cells in atherosclerotic lesions, in particular) to the liver, where the cholesterol can be exported via bile into the fecal sterol pool and removed from the body. The antiatherogenic properties of HDL have been demonstrated directly by increasing HDL levels in mice and observing reductions in the sizes of atherosclerotic lesions (4–6). In addition, HDL exerts cardioprotective effects through its antioxidant and anti-inflammatory properties (7). Recognition of the beneficial effects of increasing plasma HDL levels has increased interest in understanding the mechanism of HDL biogenesis.

HDL is formed by the interaction of apolipoprotein and ABCA1 (5, 6, 8, 9). The key role of ABCA1 in HDL metabolism is demonstrated by the fact that the mutations in this gene that lead to Tangier disease are associated with low plasma HDL levels (10). Macrophages from Tangier disease patients overaccumulate cholesterol because the ABCA1-mediated efflux of cellular free (unesterified) cholesterol (FC) and phospholipids (PLs) to apolipoprotein A-I (apoA-I) is defective. These findings are consistent with the idea that lipid transport via ABCA1 is involved in the biosynthesis of HDL particles. However, the mechanisms of ABCA1-mediated cellular PL and FC efflux are not completely understood. It is generally thought that ABCA1 functions on the surface of cells, where it either directly or indirectly translocates PL and FC to an acceptor apolipoprotein, such as apoA-I, which is the principal protein of HDL (11). ABCA1 is also present in late endosomes and lysosomes and traffics between late endosomes

and the cell surface (12). Moreover, Chen et al. (13) showed that ABCA1 has a functional role in the efflux of FC in late endosomes to apoA-I.

Before the discovery of ABCA1, Forte and colleagues (14) thoroughly characterized the HDL particles formed by CHO cells overexpressing apoA-I. They showed that the extracellular nascent apoA-I-containing particles had a range of sizes and included discoidal complexes. A similar HDL particle size distribution was observed when apoA-I was incubated with human THP-1 macrophages (15). Likewise, in our previous study, in which J774 macrophages expressing ABCA1 were incubated with human plasma apoA-I, the formation of more than one type of apoA-I-containing lipid particle was also observed (16). Similar sizes of HDL particles were observed when apoA-I was incubated with HEK293 cells (17) or CHO cells (18) transfected with ABCA1 and with several cell types, including human skin fibroblasts and CaCo-2 cells, in which ABCA1 expression was induced (18). The fact that the enhancement of ABCA1 activity in cells by either transfection or induction with agonists leads to nascent HDL particle heterogeneity is consistent with ABCA1 activity alone causing the formation of the various apoA-I-containing particles. In all cases, the major PLs incorporated into the nascent HDL particles were phosphatidylcholine (PC) and sphingomyelin (SM). Both preβ-HDL particles and α-HDL particles were observed when HepG2 cells and macrophages were incubated with apoA-I (18). These examinations of nascent HDL particles formed by ABCA1-mediated lipid efflux to apoA-I were limited in that comprehensive characterizations of the HDL particles were not conducted.

Despite the extensive studies of ABCA1 conducted in the last several years, the mechanism by which ABCA1 lipidates apoA-I and the subcellular origins of the lipids incorporated into the nascent HDL particles remain to be established. A complete biochemical characterization of the products of the ABCA1/apoA-I interaction is essential to solve the mechanism of this enzyme reaction, but this information is lacking. Here, we address this deficiency by studying the efflux of FC and PL from J774 macrophages and human skin fibroblasts in which ABCA1 is upregulated and characterizing the various nascent HDL lipid particles released into the extracellular medium. In addition, we characterize the membrane microparticles (16) that are also released from these cells by ABCA1 activity.

EXPERIMENTAL PROCEDURES

Materials

Fetal bovine serum, gentamycin, 8-(4-chlorophenyl-thio)-cAMP, and horseradish peroxidase-conjugated cholera toxin B were purchased from Sigma. BSA (essentially fatty acid-free) was obtained from Intergen Co. (Purchase, NY). [1,2-^{3}H]cholesterol (51 Ci/mmol) and [$methyl$-^{3}H]choline chloride (86 Ci/mmol) were obtained from Perkin-Elmer Life Sciences. Organic solvents were purchased from Fisher. Tissue culture dishes, flasks, and plates were from Corning, Inc. (Corning, NY) and Falcon (Lin-

coln, NJ). RPMI 1640 medium and phosphate-buffered saline were purchased from CellGro (Herndon, VA). MEM buffered with 25 mM HEPES (pH 7.4) was obtained from BioWhitaker, Inc. (Walkersville, MD). Slide-A-Lyzer mini dialysis units were purchased from Pierce (Rockford, IL). The suppliers of antibodies were as follows: rabbit polyclonal anti-mouse CD14 was purchased from Santa Cruz Biotechnology, Inc. (Santa Cruz, CA), goat polyclonal anti-human apoA-I antibody and rabbit polyclonal anti-ABCA1 antibody were purchased from Novus Biologicals (Littleton, CO), and peroxidase-conjugated Affinipure goat anti-rabbit IgG and peroxidase-conjugated Affinipure donkey anti-goat IgG secondary antibodies were purchased from Jackson ImmunoResearch (West Grove, PA).

Preparation of apoA-I

HDL was isolated from fresh plasma obtained from normolipidemic donors by sequential ultracentrifugation as described previously (19). ApoA-I was purified by anion-exchange chromatography on Q-Sepharose from HDL that was delipidated in ethanol/diethyl ether (20). The fractions containing pure apoA-I were pooled, dialyzed against 5 mM NH_4HCO_3, lyophilized, and stored at −20°C. Before radiolabeling, it was resolubilized in guanidine hydrochloride (6 M) and dialyzed extensively against labeling buffer containing 0.15 M NaCl, 0.001 M EDTA, and 0.02% NaN_3, pH 8.0. ApoA-I was radiolabeled to a specific activity of ∼1 µCi/mg by reductive methylation using [^{14}C]formaldehyde (21, 22); the formation of an average of one or fewer monomethyllysine residues per apoA-I molecule has no effect on lipid affinity (22). The protein concentration was determined by measuring its absorbance at 280 nm; the mass extinction coefficient of apoA-I is 1.13 ml/(mg × cm).

Preparation of cell monolayers

J774 mouse macrophages were routinely grown in RPMI 1640 medium containing 10% fetal bovine serum plus 0.5% gentamycin and incubated at 37°C in a humidified incubator (95% air and 5% CO_2). To collect nascent HDL particles, J774 cells were plated in 100 mm × 20 mm cell culture dishes (Corning) and grown to 80–90% confluence. Cells were then washed three times with HEPES-buffered MEM and labeled with 1 µCi/ml [^{3}H]cholesterol for 24 h or 5 µCi/ml [^{3}H]choline chloride for 48 h in RPMI 1640 medium containing 1% fetal bovine serum, as described previously (23). After labeling, cells were washed three times with MEM-HEPES, and RPMI 1640 medium containing 0.2% (w/v) BSA plus 0.3 mM 8-(4-chlorophenyl-thio)-cAMP was added to cells for 16 h to upregulate ABCA1 (23, 24). This treatment of J774 cells increased the level of ABCA1 by ∼6-fold without affecting ABCG1 levels (16). Human skin fibroblasts (GM3468A) were maintained in MEM supplemented with 10% fetal bovine serum and 0.5% gentamycin and incubated at 37°C. For lipid efflux experiments, the fibroblasts were seeded in 100 mm × 20 mm cell culture dishes, grown to confluence, and then labeled with 3 µCi/ml [^{3}H]cholesterol or 5 µCi/ml [^{3}H]choline chloride for 48 h in MEM containing 1% fetal bovine serum, as described previously (25). After labeling, the fibroblasts were washed with MEM-HEPES and incubated for 16 h in MEM containing 0.2% (w/v) BSA, 5 µg/ml 22-hydroxycholesterol, and 10 µM 9-cis-retinoic acid to upregulate ABCA1 (26); this treatment increased ABCA1 levels by ∼10-fold while having no effect on ABCG1, which was not detectable (data not shown). Some dishes from cultures of J774 macrophages and human skin fibroblasts were washed with phosphate-buffered saline, pH 7.4, dried, and extracted with isopropyl alcohol to determine the initial (t = 0) lipid levels (27). The radioactivity associated with

the extracted lipids was measured by liquid scintillation counting (16), and the amounts of PL were analyzed by phosphorus assay (28). FC mass analysis (see below) was also performed.

Efflux of cellular FC and PLs

Cells in which ABCA1 was upregulated as described above were washed with HEPES-buffered MEM, and efflux of either [^{3}H]cholesterol or [^{3}H]choline-PL was initiated by incubation with [^{14}C]apoA-I (5 μg/ml) in RPMI 1640 medium for periods of 4, 8, and 24 h. The medium was collected, centrifuged at 2,000 rpm using a Beckman Coulter Allergra™ 6R tabletop centrifuge for 10 min, and filtered through a 0.45 μm filter (Millex-HV) to remove floating cells. The radioactivity present in the incubation medium was determined by liquid scintillation counting, and the percentage of radiolabeled FC released (percentage efflux) was calculated as follows: (cpm in medium/cpm in cells at time 0) × 100. Background FC efflux (in the absence of apoA-I) was subtracted. For PL efflux, after the medium was filtered, the lipids in the medium were extracted by the procedure of Bligh and Dyer (29); the aqueous phase containing any free [^{3}H]choline was aspirated, and the chloroform phase was washed three times with 10:9 (v/v) methanol-water. The chloroform phases were pooled and dried under nitrogen in liquid scintillation vials, and [^{3}H]choline-PL radioactivity was quantitated by liquid scintillation counting. Efflux of choline-PL was calculated as described for FC efflux.

Gel filtration chromatography

Medium collected as described above and containing [^{3}H]cholesterol was not dialyzed, but medium containing [^{3}H]choline chloride was dialyzed extensively against 10 mM Tris-buffered saline, pH 7.5 (3 days with six changes of buffer) to remove excess free choline. A 3 ml aliquot of medium was loaded onto a Superdex 200 column (60 × 1.6 cm) using an Akta fast-protein liquid chromatography (FPLC) system and eluted with Tris-buffered saline plus EDTA, pH 7.5, at a flow rate of 1 ml/min. Fractions (1.0 ml) were collected, and 0.2 ml was counted to determine [^{3}H]cholesterol/[^{14}C]apoA-I or [^{3}H]choline chloride/[^{14}C]apoA-I radioactivity. The remaining 0.8 ml of relevant fractions was pooled and used to characterize the nascent HDL particles. At least three experiments were conducted to obtain complete column profiles for FC, PL, and apoA-I. To determine lipid mass in the HDL fractions, it was necessary to concentrate the conditioned medium and pooled column fractions by 10-fold using an Amicon Ultra-centrifugal filter (10,000 molecular weight cutoff). Lipids were extracted from aliquots of the concentrated medium by the method of Bligh and Dyer (29); cholesteryl methyl ether was added as an internal standard for the gas-liquid chromatographic assay of FC (30). This method can detect as little as 1.5 μg of FC. Protein was determined using a modified Lowry assay (31) for which the detection limit is 20 μg of protein. To analyze the PL subclasses present in the particles, lipids from a 250 μg PL aliquot of apoA-I-containing particles were extracted by the method of Bligh and Dyer (29) and separated by TLC using silica gel H plates with a mobile phase of chloroform-methanol-acetic acid-water (50:25:8:1, v/v). The PL bands were visualized by iodine staining, scraped, and analyzed for phosphorus using an assay (28) for which the detection limit is 2.5 μg of PL. Thus, components of the nascent HDL particles present at ≥1% of total PL could be detected.

The sizes of the lipid particles eluting in the various fractions were determined by comparing their K_{av} values with those of proteins of known diameter (particle diameter range of 6.1–17 nm). K_{av} was calculated using the following equation: $K_{av} = (V_e - V_0)/(V_t - V_0)$, where V_0 is the void volume, V_t is the total column volume, and V_e is the elution volume as described (16). A plot of log particle size against K_{av} was constructed, and the points were fitted by linear regression analysis. The particle size (hydrodynamic diameter in nm) was calculated using the following equation: $\log_{10}$ diameter $= 1.27 - 0.95\ K_{av}$ (16).

Separation of lipoproteins by two-dimensional nondenaturing gradient gel electrophoresis

Two-dimensional nondenaturing gel electrophoresis was performed on the nascent HDL particles formed in the extracellular medium as described by Asztalos and colleagues (32) with some modification. Briefly, HDL in 24 h conditioned medium was separated by charge into preβ, α, and preα mobility subclasses in the first dimension. The first dimension was prepared using 0.7% low-endosmosity agarose (Seakem LE; FMC Bio-Products, Rockford, ME) dissolved in Tris-Tricine buffer (25 mM, pH 8.6) at 95°C. The mixture was left to stand for 5 min and then poured into a mini gel cassette (1.5 mm thickness) the bottom of which was sealed with a 10% polyacrylamide gel (Mini-Protean II Cell; Bio-Rad, Hercules, CA); a 10-well comb (1 mm thickness) was placed on top of the gel for 30 min while the gel hardened. Samples (40 μl; containing 4–8 μg of apoA-I) were mixed with 10 μl of Tris-Tricine buffer containing 50% glycerol plus 1% bromophenol blue, loaded into the wells, and electrophoresed at constant voltage (100 V for 2.5 h) at 4°C. The agarose strips were excised and transferred onto the top of nondenaturing 2–36% concave gradient polyacrylamide gels that were prepared using a 2:1 (v/v) ratio of the 2% and 36% polyacrylamide solutions (32) in a gradient maker (model 395; Bio-Rad, Richmond, CA). HDL samples were electrophoresed in the second dimension at 50 V (4°C) for 18–20 h. Gels were removed and incubated in transfer buffer containing 200 mM glycine and 20 mM Tris for 10 min. Proteins on the gel were then transferred onto polyvinylidene difluoride membranes using the semidry blotting procedure (Bio-Rad). The polyvinylidene difluoride membranes were then blocked with 5% rabbit serum in Tris-buffered saline (20 mM Tris and 500 mM sodium chloride, pH 7.5) containing 0.05% Tween 20 for 1 h. The membranes were then washed three times (10 min each) with the same buffer and incubated with human polyclonal apoA-I antibody at 1:5,000 dilution. After three more washes, the membranes were incubated for 1 h with a peroxidase-conjugated Affinipure donkey anti-goat IgG secondary antibody at 1:50,000 dilution in the same buffer. After additional washes with the Tween 20-containing buffer, the membrane was incubated with a chemiluminescence reagent according to the manufacturer's protocol (Bio-Rad) and exposed to BioMax film (Kodak).

The diameters of the nascent HDL particles from the Western blot were determined by comparing their relative mobility (R_f) values with those of standard molecular markers of known diameter (particle diameter range of 4.7–17 nm). A calibration plot of log particle size against R_f was constructed, and the points were fitted by linear regression analysis; the particle size (nm) from the Western blot was calculated using the following equation: $\log_{10}$ diameter $= 1.54 - 0.92\ R_f$.

Isolation of nascent HDL particles and chemical cross-linking

To assess the number of apoA-I molecules per HDL particle, bis(sulfosuccinimidyl) suberate (BS^3) was used to chemically cross-link the apoA-I molecules within the particles. Briefly, HDL-containing fractions from FPLC were adjusted to a density of 1.21 g/ml with KBr and centrifuged in a Beckman Ti 70.2 rotor at 50,000 rpm for 24 h at 4°C to isolate the nascent HDL particles. At the end of the centrifugation, the sample was separated into 1 ml fractions. A sample (0.1 ml) of each fraction was dialyzed three

times per hour against deionized water using a Slide-A-Lyzer mini dialysis unit and counted for [³H]cholesterol/[¹⁴C]apoA-I to determine the presence of HDL particles. The fractions containing the nascent HDL particles were then pooled and dialyzed three times against 0.1 M phosphate buffer, pH 7.4, and concentrated to 0.5–1 mg/ml apoA-I using an Amicon Ultracentrifugal filter. Particles were then incubated with BS^3 (10 mM) in 0.1 M phosphate buffer, pH 7.4, at room temperature for 3.5 h, and the reaction was quenched with 25 mM ethanolamine. The samples were then subjected to 4–20% gradient SDS-PAGE and stained with Coomassie blue to visualize the apoA-I bands. The degree of apoA-I oligomerization was assessed by comparison with standards of known molecular weight.

Circular dichroism spectroscopy

Circular dichroism spectra were recorded from 184 to 260 nm at room temperature using a Jasco J-600 spectropolarimeter. Purified nascent HDL particles were isolated as described above and concentrated to 15 μg/ml apoA-I in 10 mM sodium phosphate buffer (pH 7.4), and the circular dichroism spectrum was obtained. The results were corrected by subtracting the buffer baseline, and the α-helix content was calculated from the molar ellipticity at 222 nm, as described (33).

Electron microscopy

Nascent HDL particles were prepared as mentioned above, concentrated to 1–2 mg/ml apoA-I, and dialyzed against 0.125 M ammonium acetate, 2.6 mM ammonium carbonate, and 0.26 mM tetrasodium EDTA, pH 7.4, at 4°C overnight. The sample was then negatively stained with 2% sodium phosphotungstate and examined with a Zeiss 10A electron microscope, as described (34).

Detection of CD14 and ganglioside in microparticles

After FPLC, void volume fractions containing microparticles released by the cells were pooled and further purified by adjustment to 1.21 g/ml with KBr and centrifugation in a Beckman Ti 70.2 rotor at 50,000 rpm for 24 h at 4°C. The centrifuged solution was fractionated, and the fractions were each dialyzed three times per 8 h against 0.1 M Tris-HCl buffer, pH 7.5. The fractions containing microparticles were then located by counting for [³H]cholesterol. Proteins in the microparticles were separated using 4–15% gradient SDS-PAGE. The separated proteins were transferred onto nitrocellulose membranes with a semidry electrophoretic transfer apparatus using transfer buffer (0.1 M Tris, 0.192 M glycine, and 20% methanol). The membranes were blocked with 5% nonfat milk in Tris-buffered saline containing 0.1% Tween 20 for 1 h. To detect CD14 and ABCA1, the membrane was probed with either rabbit polyclonal anti-mouse CD14 antibody (1:200 dilution) or rabbit polyclonal anti-ABCA1 antibody (1:1,000 dilution) followed by peroxidase-conjugated Affinipure goat anti-rabbit IgG (1:50,000 dilution). Horseradish peroxidase-conjugated cholera toxin B (5 ng/ml) was used to detect ganglioside (GM_1) (35). CD14 and GM_1 bands were visualized by chemiluminescence.

RESULTS

Characterization of the nascent HDL particles formed by J774 macrophages

Figure 1 shows the Superdex 200 gel filtration fractionation of the lipid particles present in the extracellular medium after incubation of J774 macrophage cells with
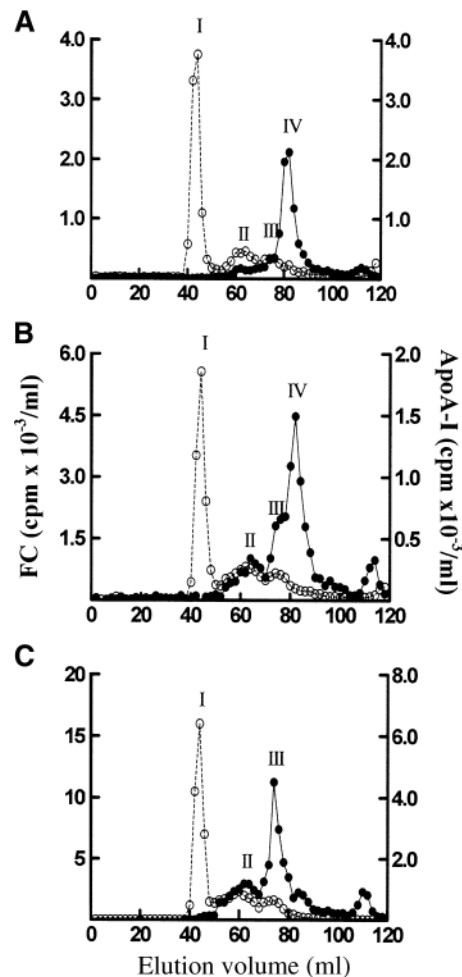
Fig. 1. Gel filtration elution profiles of medium collected after 4, 8, and 24 h incubations of cAMP-stimulated J774 macrophage cells with [¹⁴C]human plasma apolipoprotein A-I (apoA-I). J774 mouse macrophage cells were labeled with [³H]cholesterol and treated with 8-(4-chlorophenyl-thio)-cAMP as described in Experimental Procedures. [¹⁴C]human plasma apoA-I (5 μg/ml) was added to the cells. After 4 h (A), 8 h (B), and 24 h (C) incubations at 37°C, media were collected, processed as described in Experimental Procedures, and subjected to Superdex 200 gel filtration chromatography. Fractions were collected, and radioactivity was determined by liquid scintillation counting. Open circles, [³H]cholesterol; closed circles, [¹⁴C]human plasma apoA-I. The void volume of the column was 44.4 ml, and the total volume was 116.8 ml. For each incubation time, one representative profile is shown from three independent experiments. FC, free (unesterified) cholesterol.

apoA-I (5 μg/ml) for 4, 8, and 24 h. It is apparent that FC is present in peaks I, II, and III at each time point and that the peaks have constant elution volumes (cf. Fig. 1A, B, C). The elution volumes of peaks I, II, and III are 44.4, 62, and 74 ml, respectively. The K_{av} values indicate that the hydrodynamic diameter of particles in peak I is >20 nm, whereas the diameters of the particles in peaks II and III are ~12 and 9 nm, respectively. These particle sizes are similar to those reported previously (16). **Table 1** shows the distribution of the FC released from J774 macrophages between column fractions as a function of time. It is im-

TABLE 1. Distribution of [³H]cholesterol and [³H]choline-PLs released from J774 macrophages between FPLC fractions as a function of time

Incubation Time	Percent Total Cell Efflux[a]	Percent Effluxed [³H]Cholesterol[b]			Percent Effluxed [³H]Choline-PL[b]		
		Peak I	Peak II	Peak III	Peak I	Peak II	Peak III
4 h	8 ± 2	57 ± 6	18 ± 9	11 ± 7	52 ± 9	23 ± 11	16 ± 10
8 h	13 ± 2.5	50 ± 8	21 ± 12	14 ± 10	30 ± 11	36 ± 12	23 ± 9
24 h	18 ± 1.5	51 ± 11	24 ± 14	15 ± 12	11 ± 11	52 ± 9	33 ± 10

apoA-I, apolipoprotein A-I; FPLC, fast-protein liquid chromatography; PL, phospholipid.

[a] Percent cell [³H]cholesterol efflux to 5 µg/ml apoA-I was calculated by comparing the total amount of [³H]cholesterol released at 4, 8, and 24 h with the total [³H]cholesterol in the J774 macrophages at time 0 (n = 3). Efflux to medium in the absence of apoA-I was subtracted at each time point.

[b] Percent effluxed [³H]cholesterol and [³H]choline-PL values are means ± SD from three independent experiments. Gel filtration elution profiles of the type shown in Fig. 1 were analyzed. The percentage distributions relate to the material eluted from the column at 40–90 ml. The typical overall recoveries of [³H]choline-PL, [³H]cholesterol, and [¹⁴C]apoA-I from the column were ~60, 70, and 80%, respectively.

portant to note that peak I contains at least 50% of the effluxed FC and that the distribution of FC between peaks I, II, and III does not change significantly with time. This is consistent with the parallel release of FC into the particles that constitute peaks I–III. The ratios of FC to apoA-I cpm in peaks II and III remain unchanged as the time of incubation of apoA-I with the cells increases from 4 to 24 h. This implies that the compositions of the 12 and 9 nm nascent HDL particles do not change over this time frame.

Table 1 also reveals how the acquisition of cellular choline-PL by apoA-I proceeds with time. The relative amount of [³H]choline-PL in peak I decreases with time, whereas the proportions in peaks II and III increase as the apoA-I cell contact period increases. The PL radioactivity associated with peaks II and III increases over the 4–24 h period, with the peak II/III ratio remaining constant at ~1.5 (Table 1). The fractions of [³H]choline-PL associated with peak I decrease with time, indicating that there is preferential release of radiolabel into peaks II and III particles at longer incubation times. It should be noted that apoA-I cannot create HDL-like particles by solubilizing peak I material (16). To explore this point further, some cells were incubated with 5 µg/ml apoA-I for 4 h; after removal from cells, half of the medium was analyzed immediately by FPLC and the other half was incubated at 37°C for a further 20 h before FPLC analysis. The two FPLC profiles were the same, indicating that the particles do not reorganize during 20 h of incubation at 37°C. Overall, these results are consistent with the idea that there is no precursor-product relationship between the peaks I, II, and III particles. In contrast, there is a precursor-product relationship between the unreacted lipid-free apoA-I in peak IV and that eluting in peaks II and III. Thus, at 4 h, most of the apoA-I is in peak IV, with very little in peaks II and III (Fig. 1A). Comparison of Fig. 1B and C indicates that there is a progressive shift of apoA-I into peaks II and III at longer incubation times. After 24 h, peak III contains most of the apoA-I (Fig. 1C), and the disappearance of peak IV indicates that essentially all of the free apoA-I (5 µg/ml) added to the cells is consumed in the creation of the peaks II and III nascent HDL particles.

To determine the electrophoretic mobilities and further examine the sizes of the nascent HDL particles

formed by incubating apoA-I with J774 macrophages, 24 h conditioned medium was subjected to two-dimensional nondenaturing Western blot analysis (**Fig. 2A**). It is apparent that most of the apoA-I is present in α-migrating HDL particles; the preβ band is free apoA-I or lipid-poor apoA-I. The mobility of these particles was assigned relative to a BSA standard that possesses α mobility. Based on their R_f values, the diameters of the three nascent α-HDL bands are 14, 12, and 8.5 nm. These sizes are consistent with the
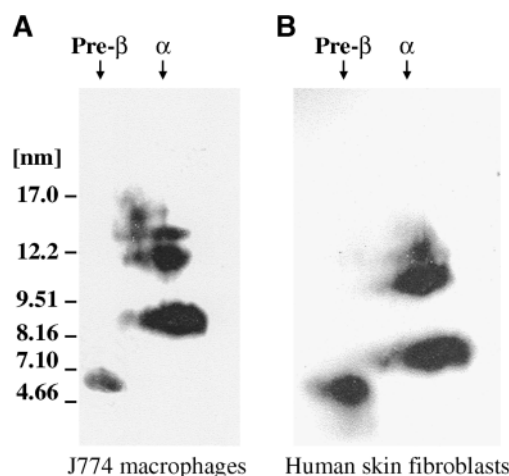
Fig. 2. Western blot analysis of two-dimensional native gel electrophoresis of apoA-I-containing nascent HDL particles generated by incubation of J774 macrophages and human skin fibroblasts with human plasma apoA-I. After incubation of J774 mouse macrophages and human skin fibroblasts with human plasma apoA-I (5 µg/ml) for 24 h at 37°C, media were collected and prepared as described in Experimental Procedures. Ten micrograms of apoA-I-containing particles from each medium was electrophoresed in the first dimension on a 0.7% agarose gel, followed by electrophoresis in the second dimension on a 2–36% concave polyacrylamide gel (see Experimental Procedures). The nascent HDL bands from the two-dimensional gel were transferred onto a polyvinylidene difluoride membrane via a semidry blot system and probed with a polyclonal anti-apoA-I antibody. A: J774 macrophage whole medium. B: Human skin fibroblast whole medium. Molecular size markers (diameter in nm) are indicated. The HDL particle diameters are derived from the relative mobility values of the centers of the various bands; the widths of the bands typically span a diameter range of ±0.8 nm.

TABLE 2. PL composition of microparticles and nascent HDL particles formed by incubation of apoA-I with J774 macrophages

Column Fraction	Hydrodynamic Diameter[a]	Percent of Total PLs[b]					
		PC	SM	Lyso-PC	PE	PS	PI
		nm					
Peak I	>20	37 ± 3	12 ± 5	8 ± 4	13 ± 5	16 ± 3	14 ± 2
Peak II	12 ± 0.4	43 ± 3	15 ± 1	6 ± 4	14 ± 2	10 ± 2	12 ± 1.5
Peak III	9 ± 0.5	66 ± 5	9 ± 2	4 ± 1	7 ± 2	5 ± 2	9 ± 2

PC, phosphatidylcholine; PE, phosphatidylethanolanime; PI, phosphatidylinositol; PS, phosphatidylserine; SM, sphingomyelin.

[a] Molecular mass and particle diameter of an equivalent globular protein were derived using the calibration equations described in Experimental Procedures. Data are shown as means ± SD from three independent experiments.

[b] Percentages of total PL were obtained from four independent experiments using TLC and phosphorus analysis. Values shown are means ± SD (n = 4). Comparison by one-way ANOVA of the levels of PC, SM, lyso-PC, PE, PS, and PI in the 12 and 9 nm HDL particles indicates the following significant differences: $P < 0.001$, $P > 0.05$, $P > 0.05$, $P < 0.05$, $P < 0.05$, and $P > 0.05$, respectively.

diameters calculated for the peaks II (contains 12 nm nascent HDL particles predominantly, plus small amounts of 14 nm particles) and III (contains 9 nm nascent HDL particles) fractions shown in the FPLC elution profile (Fig. 1). Examination of the pooled peak II and III fractions by Western blotting showed that at least 80% of the apoA-I was present in the major HDL particle expected for each fraction (data not shown).

Because the nascent HDL particles possess α-electrophoretic mobility, it is possible that acidic lipids contribute to the particle negative charge. To address this issue, the lipid compositions of these particles were analyzed. **Table 2** shows the distribution of PL in the 9 and 12 nm nascent HDL particles as established by TLC and phosphorus analysis. Lyso-PC is present (Table 2) together with some free fatty acid (the levels are similar to those reported for lyso-PC; data not shown). PC is the predominant PL in both the 9 and 12 nm particles, but the particles contain significantly different ratios of PC and SM. The PC/SM ratios are ~7:1 and 3:1 for the 9 and 12 nm nascent HDL particles, respectively. Apart from the PC, phosphatidylethanolamine (PE), and phosphatidylserine (PS) contents, the levels of the remaining PL classes are the same for both sizes of HDL particles. The fact that the PL compositions of the 9 and 12 nm nascent HDL particles formed

by J774 macrophages are different also raises the possibility that there are differences in the amounts of PL, FC, and apoA-I per particle. The results of mass analyses to address this point are summarized in **Table 3**; it is apparent that the 12 nm particle is relatively FC-rich, with a FC/PL molar ratio of 1:5 compared with a ratio of 1:8 for the 9 nm HDL. Chemical cross-linking of the apoA-I molecules in the 9 and 12 nm HDL particle fractions (**Fig. 3**) shows that the smaller 9 nm HDL particles contain two apoA-I molecules, whereas the larger HDL particles contain three or four apoA-I molecules per particle. These results are consistent with the two-dimensional Western blot (Fig. 2), in which the 8.5 nm HDL fraction appears as a single α-band and the 12 nm fraction appears as a doublet α-band. The secondary structure of apoA-I in the 9 and 12 nm HDL particles is similar. Thus, far-ultraviolet circular dichroism measurements show that the apoA-I α-helix contents are ~50% in both cases (Table 3); no other protein bands besides apoA-I were apparent by silver-stained SDS-PAGE of concentrated samples (data not shown).

Figure 4 shows the morphology of the isolated and purified 9 and 12 nm HDL particles as determined by electron microscopy. Both the 9 and 12 nm HDL particles form rouleaux, which are characteristic of discoidal lipoprotein particles that constitute a segment of PL bilayer.

TABLE 3. Characteristics of nascent HDL particles formed by incubation of apoA-I with J774 macrophages

Column Fraction[a]	Hydrodynamic Diameter[b]	ApoA-I Number[c]	Composition (PL/FC/apoA-I)[d]	α-Helix Content[e]
	nm	mol/particle	mol/mol	%
Peak II	12 ± 0.4	3–4	195 ± 7:39 ± 4:1	54 ± 5
Peak III	9 ± 0.5	2	96 ± 4:12 ± 1:1	49 ± 4

FC, free (unesterified) cholesterol.

[a] The cells were treated and the medium fractionated as described for Fig. 1.

[b] Particle diameters were obtained as described in Table 2.

[c] Numbers of apoA-I molecules per nascent HDL particles were obtained by cross-linking apoA-I with bis(sulfosuccinimidyl) suberate.

[d] The compositions of the pooled fractions from each peak from the FPLC (Fig. 1) were determined using mass analysis of lipids and apoA-I (see Experimental Procedures). Values are means ± SD from three independent experiments.

[e] The secondary structural characteristics of apoA-I in peaks II and III were obtained by calculating the percentage of α-helix content using far-ultraviolet circular dichroism spectra (see Experimental Procedures). Data shown are from two to three independent experiments.
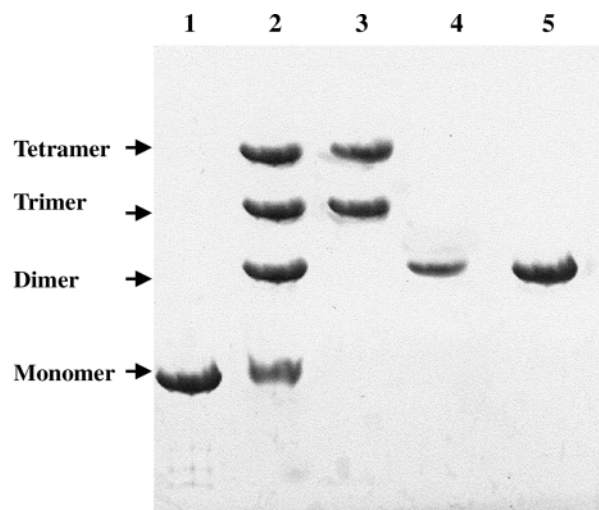
Fig. 3. Chemical cross-linking with bis(sulfosuccinimidyl) suberate (BS[3]) of apoA-I in nascent HDL particles released from J774 macrophages. Pooled fractions of peaks II and III (containing 9 and 12 nm nascent HDL particles, respectively) from fast-protein liquid chromatography (FPLC) were adjusted to a density of 1.21 g/ml with KBr and centrifuged in a Beckman Ti 70.2 rotor at 50,000 rpm for 24 h at 5°C to isolate the 9 and 12 nm nascent HDL particles. The purified particles were dialyzed three times against 0.1 M phosphate buffer, pH 7.4, concentrated to 0.5–1 mg/ml apoA-I using an Amicon Ultra-centrifugal filter, and then incubated with BS[3] (10 mM) in 0.1 M phosphate buffer, pH 7.4, at room temperature. The cross-linked nascent HDL particles were separated using 4–20% gradient SDS-PAGE and stained with Coomassie blue. Lane 1, lipid-free apoA-I (applied, 5 µl; containing 2 µg of apoA-I); lane 2, lipid-free apoA-I plus BS[3] (applied, 15 µl; containing 15 µg of apoA-I); lane 3, 12 nm nascent HDL particles plus BS[3] (applied, 30 µl; containing 15 µg of apoA-I); lane 4, 9 nm nascent HDL particles plus BS[3] (applied, 35 µl; containing 10 µg of apoA-I); lane 5, apoA-I/POPC (1:100 mol/mol) reconstituted discoidal HDL plus BS[3] (applied, 15 µl; containing 15 µg of apoA-I). Positions of monomers, dimers, trimers, and tetramers were assigned according to their calculated molecular weights.

These discoidal HDL particles have mean major diameters of 9 ± 2 and 12 ± 2 nm. These results are consistent with the sizes determined by gel filtration chromatography (Fig. 1) and two-dimensional nondenaturing gel electrophoresis (Fig. 2A).

### Characterization of microparticles formed by J774 macrophages

As shown in Fig. 1 and Table 1, a large amount of the radiolabeled FC released by J774 macrophages is present in the peak I fraction, which contains >20 nm diameter particles that elute in the void volume when analyzed by FPLC gel filtration. To further examine the size of these particles, electron microscopy was used (**Fig. 5**), and the average diameter of the particles was measured as 24 ± 2 nm. The particle morphology is quasispherical, in marked distinction to the disc-shaped nascent HDL particles (Fig. 4). The composition of these microparticles is summarized in Table 2. Both the FC content and PL class distribution are similar to those observed for the larger 12 nm HDL particles (cf. Tables 2, 3). The PC/SM ratio of ~3 is

lower than that of the 9 nm HDL particles that are released concurrently from the cells.

We examined the protein composition of the microparticles to gain more insight into their subcellular origin. **Figure 6** shows that the microparticles contain multiple proteins ranging in molecular mass from 15 to 150 kDa. Importantly, a Western blot probed for CD14, the monocyte differentiation antigen that is present in microparticles released from such cells (36), indicates that the microparticles contain this glycosylphosphatidylinositol-anchored protein (band a in Fig. 6). In addition, probing with cholera toxin B shows that the microparticles contain GM$_1$ (band b in Fig. 6). The microparticles do not contain detectable levels of ABCA1. ApoA-I is not required for the release of microparticles (16), and the affinity of apoA-I for the surface of the microparticles is low because, under the experimental conditions used in this study, apoA-I is not detected in the peak I fraction.

Influence of cell type

We made parallel measurements with human skin fibroblasts to compare the lipid particles released by different cell types. The procedures to prepare the cells and isolate
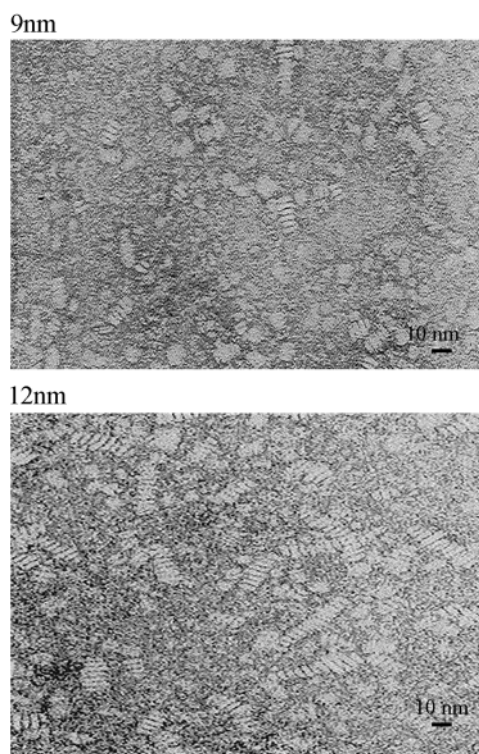
Fig. 4. Electron micrographs of negatively stained nascent HDL particles from J774 macrophages. Pooled fractions from peaks II and III from FPLC (see Fig. 1) were adjusted to a density of 1.21 g/ml with KBr and centrifuged as described for Fig. 3 to isolate the nascent HDL particles. Purified 9 and 12 nm nascent HDL particles were dialyzed against 0.125 M ammonium acetate, 2.6 mM ammonium carbonate, and 0.26 mM tetrasodium EDTA at pH 7.4 to remove KBr and concentrated to 0.5–1 mg apoA-I/ml. The electron microscopic analysis was performed as described in Experimental Procedures. A: 9 nm nascent HDL particles. B: 12 nm nascent HDL particles. Bars = 10 nm.
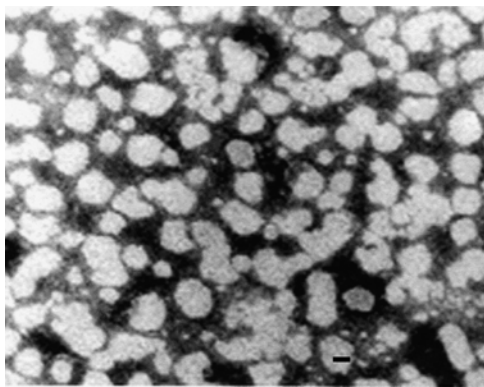
**Fig. 5.** Negative stain electron micrograph of microparticles released from J774 macrophage cells. After FPLC (see Fig. 1), peak I fractions were pooled, adjusted to a density of 1.21 g/ml with KBr, centrifuged at 50,000 rpm in a Beckman 70.1 Ti rotor, and dialyzed as described for Fig. 4 to isolate the microparticles. The electron microscopic analysis was performed as described in Experimental Procedures. Bar = 10 nm.

lipid particles were similar to those used with J774 macrophages. **Figure 7** shows the FPLC profile of the medium obtained with human skin fibroblasts that were labeled with [^{3}H]choline chloride and incubated with [^{14}C]apoA-I (5 μg/ml). As observed with J774 macrophages (Fig. 1),
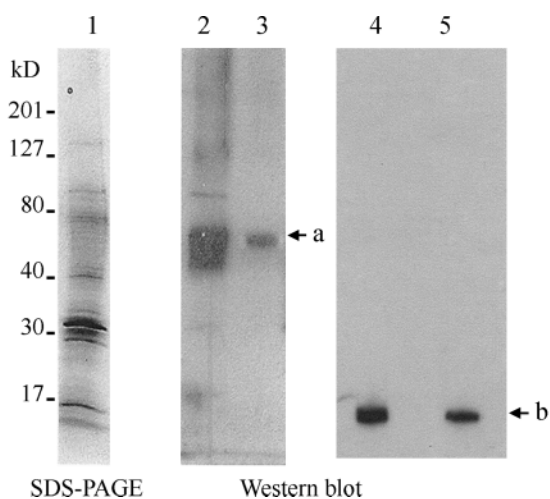
Fig. 6. SDS-PAGE and Western blot analysis of proteins and ganglioside (GM$_1$) in microparticles formed by J774 macrophages. Microparticles from peak I of FPLC (see Fig. 1) were isolated at a density of 1.21 g/ml (see Experimental Procedures). Proteins from the microparticles and cell lysate were separated using a SDS-PAGE 4–15% gradient gel, and Western blotting was performed using CD14 antibody (Santa Cruz Biotechnology) at a 1:200 dilution followed by anti-IgG horseradish peroxidase-conjugated secondary antibody (Jackson Immunoresearch Laboratories, Inc., Jacksonville, PA) at a 1:50,000 dilution to detect CD14. Horseradish peroxidase-conjugated cholera toxin B (5 ng/ml) was used to detect GM$_1$. CD14 and GM$_1$ bands were visualized by chemiluminescence. Lane 1, isolated microparticles were analyzed by SDS-PAGE and stained with Coomassie blue; lanes 2 and 3, Western blots of cell lysate and microparticles, respectively, probed with anti-CD14 (a indicates the CD14 band); lanes 4 and 5, Western blots of cell lysate and microparticles, respectively, probed with cholera toxin B (b indicates the GM$_1$ band).
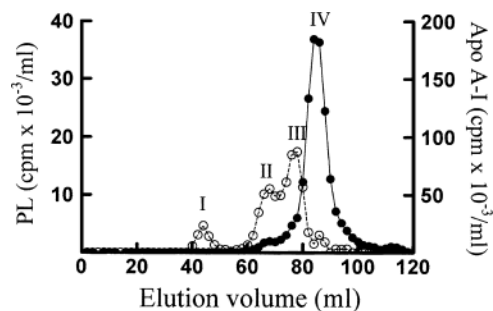
Fig. 7. Gel filtration elution profile from medium collected after a 24 h incubation of human fibroblasts in which ABCA1 was upregulated with [^{14}C]human plasma apoA-I. Wild-type human fibroblasts were labeled with [^{3}H]choline chloride for 48 h and treated with 22-(R) hydroxylcholesterol and 9-*cis*-retinoic acid to upregulate ABCA1, as described in Experimental Procedures. [^{14}C]apoA-I (5 μg/ml) was added to the labeled cells and incubated for 24 h. The medium was collected and analyzed as described for Fig. 1. Open circles, [^{3}H]choline phospholipids (PL); closed circles, [^{14}C]human plasma apoA-I.

the microparticles eluting at a void volume of 44.4 ml do not contain apoA-I. However, HDL fractions II and III, which have elution volumes of 68 and 78 ml, respectively, contain apoA-I and elute later than corresponding fractions from J774 macrophages (Fig. 1). This indicates that human skin fibroblasts form smaller nascent HDL particles than those from J774 macrophages: the hydrodynamic diameters of the peaks II and III particles are 11 and 8 nm, respectively. The Western blot shown in Fig. 2B confirms that the fibroblast nascent HDL particles are smaller than the J774 nascent HDL particles (Fig. 2A). The diameters of the fibroblast HDL particles from the Western blot are 13, 11, and 7.5 nm. As seen with J774 macrophages, the larger nascent HDL particles appear as a doublet in the two-dimensional Western blot (Fig. 2B). Comparison of the 24 h choline-PL distributions listed in Table 1 and **Table 4** indicates that the relative amounts of large and small HDLs created by fibroblasts and J774 cells are different, with the ratios of peaks II and III being ∼0.7 and 1.6, respectively. The human skin fibroblast nascent HDL particles have different FC contents compared with their J774 counterparts: the FC/PL molar ratios are 1:12 and 1:4 for the 11 and 8 nm HDL particles from fibroblasts (**Table 5**) and 1:5 and 1:8 for the 12 and 9 nm nascent HDL particles from J774 macrophages (Table 3). The microparticles of human skin fibroblasts have a FC/PL

TABLE 4. Distribution of [^{3}H]choline-PLs released from human skin fibroblasts incubated with [^{14}C]human plasma apoA-I (5 μg/ml) for 24 h

Time	Percent Effluxed [^{3}H]Choline-PL		
	Peak I	Peak II	Peak III
24 h	10 ± 3	33 ± 3	48 ± 2

Values were obtained from three independent experiments using 24 h conditioned medium produced by human skin fibroblasts. The peaks were isolated after fractionation using FPLC as described in Experimental Procedures.

TABLE 5. Characteristics of nascent HDL particles formed by ABCA1/apoA-I interaction in human skin fibroblasts

Column Fraction	Hydrodynamic Diameter	Composition (PL/FC/apoA-I)
	nm	mol/mol
Peak I	>20	
Peak II	11 ± 0.6	95 ± 3:8 ± 2:1
Peak III	8 ± 0.4	25 ± 4:6 ± 2:1

Values were obtained as described in Table 3 and are means ± SD (n = 3).

molar ratio of 0.5 and a PL/protein mass ratio of 0.03, compared with values of 0.22 and 0.2, respectively, for microparticles from J774 cells. Approximately one-third of the total FC appearing in the extracellular medium is associated with the microparticles that elute in the column void volume (Fig. 7) (data not shown).

DISCUSSION

The major source of plasma HDL is ABCA1-expressing cells in the liver (1, 37, 38). Although the ABCA1-mediated production of HDL particles from macrophages represents only a tiny fraction of total plasma HDL, it is the most important with regard to reducing atherosclerosis (6). Despite its significance and many studies, the mechanism of ABCA1-mediated efflux of cellular lipids to form HDL particles remains unclear. The goal of this study was to clarify the situation by focusing on the characterization of the nascent HDL particles formed by the interaction of apoA-I with ABCA1 (39, 40).

Nascent HDL

In agreement with prior results from this laboratory (16) and others (17, 18, 41), a heterogeneous population of differently sized nascent HDL particles is created when ABCA1 in J774 macrophages and human skin fibroblasts exports PL and FC to apoA-I (Figs. 1, 2, 7). The predominant HDL species are discoidal in shape (Fig. 4), have hydrodynamic diameters of ~9 and 12 nm, and possess α-electrophoretic mobility (Fig. 2). Because both lipid-free apoA-I and apoA-I/PC discoidal complexes exhibit preβ-electrophoretic mobility, the extra negative surface charge leading to α-mobility arises from the presence of acidic PS and phosphatidylinositol molecules (and free fatty acids) in the nascent HDL particles (Table 2) (42). The ability of cellular acidic PL to induce α-electrophoretic mobility in apoA-I-containing lipoprotein particles has been demonstrated with fibroblasts (43) and other cell types (14, 15). The apoA-I-containing particles with preβ-electrophoretic mobility (Fig. 2) require further characterization; this band may contain a mixture of lipid-free apoA-I and small lipid-poor particles that are not resolved on the two-dimensional gel. Importantly, apoA-I-containing nascent HDL particles are not the only FC/PL particles released into the extracellular medium by the activity of ABCA1. At least half of the cellular FC effluxed from J774 cells during a 24 h incubation with apoA-I (Table 1) is present in the extracellular medium as apoA-I-free microparticles (see below). In our system, the FC and PL efflux simultaneously from the cell (44) and microparticles and the various nascent HDL particles are created concurrently, as reflected by the lack of evidence for a precursor-product relationship between peaks I, II, and III. The lipid particles in these three fractions are stable, as reflected by the lack of change in composition during the 24 h cellular incubations. This observation indicates that there is no significant remodeling attributable to the secretion of any lipid transfer proteins from the J774 cells. As discussed further below, these various lipid particles are probably the products of ABCA1 molecules located in different cell membrane microenvironments.

Previous analyses of the lipids present in conditioned medium from ABCA1-expressing cells incubated with apoA-I have been for the total medium rather than for the separated microparticles and nascent HDL fractions. The compositions listed in Table 3 indicate that, as expected, the larger 12 nm particle contains more apoA-I molecules and is relatively lipid-rich. The PL/apoA-I ratios are greater than those based on choline-PL specific radioactivity reported previously by us (16); the current mass analyses include all PL classes and are not affected by any variations in the specific radioactivity of different cellular pools of choline-PL. The overall composition and apoA-I α-helix content are generally consistent with models of discoidal HDL particles obtained from in vitro reconstitution experiments. Thus, both the 9 and 12 nm nascent HDL particles constitute a segment of PL bilayer stabilized by the amphipathic α-helices of apoA-I arranged in a belt-like manner around the edge of the disc (45). The larger 12 nm HDL particle released from J774 macrophages is FC-enriched relative to its 9 nm counterpart (Table 3) (16, 17). The major nascent HDL species from J774 cells contain two or three apoA-I molecules per particle, and apoA-I is the only apolipoprotein detected. J774 macrophages are unusual in that they do not express apoE. The human macrophage cell line, THP-1, does express apoE, and we have also observed a heterogeneous distribution of nascent HDL sizes with this cell type (our unpublished data). The effect of endogenous apoE on the particle size distribution in this case is not known, but the assembly of apoA-I-containing nascent HDL particles has been shown to predominate with THP-1 cells (15).

The fact that the 9 and 12 nm nascent HDL particles have different PL compositions (Table 2) supports the concept that the lipids in these particles originate from different subcellular locations. The distribution of PL classes in the 9 nm particle is similar to that found in human HDL_2 and HDL_3 (11). In contrast, the nascent 12 nm particle is relatively depleted in PC and enriched in amino-PL (PE + PS), implying that significant remodeling of the PL would occur in plasma to create mature HDL particles. The lyso-PC contents of the nascent HDL particles are in the range observed with mature HDL_2 and HDL_3. It is intriguing that lyso-PC is the only PL of those listed in Table 2 that has been shown to have the ability to form a defined molecular complex with apoA-I (4 mol/mol apoA-I) (46). Further work will be

required to determine whether this low level of lyso-PC plays a critical role in the process of lipidation of apoA-I by ABCA1.

A striking feature of the nascent HDL PL compositions in Table 2 is that the PC/SM ratios are ∼7:1 and 3:1 for the 9 and 12 nm particles, respectively. The relative enrichment of SM and FC in the 12 nm particle is consistent with it originating from a liquid-ordered membrane raft domain (47). The enrichment of PC in the 9 nm particle implies that it originates from a relatively disordered membrane domain. The high level of choline-PL (PC + SM) and the low level of amino-PL (PE + PS) suggest that the lipids recruited into the 9 nm nascent HDL particle mostly originate from the exofacial leaflet of the plasma membrane. Indeed, the PE and PS may also be derived from the same locus, because ABCA1 has the ability to translocate PS and PE across the membrane (48, 49). In contrast, the reduced level of PC and the enhanced levels of PE and PS in the 12 nm HDL particle (Table 2) may reflect the recruitment of lipids from both leaflets of membrane rafts. These considerations relate to the incorporation of plasma membrane lipids into the nascent HDL particles. However, ABCA1 is known to traffic between the plasma membrane and late endosomal/lysosomal membranes (12, 13, 50) such that intracellular FC (13, 51), and that in late endosomes in particular (13, 52), is a substrate for efflux via ABCA1. Because ABCA1 mediates the retro-endocytosis of apoA-I (52, 53) and the late endosomal membrane does not contain much FC (54), it is possible that the late endosomal membrane may be the major site of origin of the lipids present in the 9 nm nascent HDL particle. Further work is required to elucidate the intermediate states that lipid-free apoA-I molecules pass through after they interact with ABCA1 and are converted into the discoidal nascent HDL particles described here.

Microparticles

Examination of Table 2 indicates that the PL compositions of microparticles released from J774 cells and the 12 nm nascent HDL particles are the same. Thus, the PL in microparticles probably originates from plasma membrane raft domains. The size of the microparticles (Fig. 5) and the presence of multiple proteins (Fig. 6) are consistent with the microparticles being plasma membrane vesicles (55, 56). Such particles are reported to contain proteins both in the membrane and the aqueous interior; this explains the low PL/protein ratios that we measured, with the lower value for fibroblast microparticles perhaps reflecting a relatively high content of cytoskeletal elements. Because the microparticles contain the glycosyl-phosphatidylinositol-anchored CD14 molecule and the GM$_1$ (Fig. 6), both of which are markers of plasma membrane rafts (36, 57), it is likely that the vesiculation to release the microparticles involves plasma membrane raft domains. It is thought that the externalization of plasma membrane PS by ABC transporters in activated cells leads to microparticle shedding (58). Because ABCA1 can induce such transmembrane migration of PS (48, 49), it is reasonable to expect ABCA1 activation to promote the concomitant release of microparticles from the plasma membrane and the formation of nascent HDL particles. ABCA1 may also promote exocytosis (59), but because exosomes have low contents of CD14 (60) and the J774 microparticles have abundant CD14 (Fig. 6), it seems unlikely that export of membrane vesicles from the cell interior is responsible for the microparticle formation in our system. The involvement of ABCA1 in microparticle production is supported by the observation that the number of microparticles in the plasma of ABCA1-null mice is lower than that in wild-type animals (61). This observation implies that microparticles created by ABCA1 activity enter the circulation. Finally, it is notable that microparticles have procoagulant activity (58), so there may be a negative aspect to their production by activation of ABCA1. This is in contrast to the beneficial effects expected by the increased production of antiatherogenic nascent HDL particles.

Comparison of J774 macrophages and human skin fibroblasts

Fibroblasts in which ABCA1 activity is upregulated behave similarly to J774 cells in that incubation with apoA-I gives rise to a heterogeneous distribution of nascent HDL particles (Figs. 2, 7). In contrast with macrophages, fibroblasts do not secrete proteins such as apolipoproteins or lipid transfer proteins that can remodel lipoproteins. Because no evidence of nascent HDL particle remodeling was observed with either cell type, it follows that the observed HDL particle heterogeneity is a direct consequence of ABCA1 activity, presumably in different membrane microenvironments. We have noted that FC loading of cells leads to the formation of larger, FC-enriched nascent HDL (16), so differences in membrane FC content may contribute, in part, to the smaller HDL particles that have relatively low FC/apoA-I molar ratios created with human skin fibroblasts (cf. Tables 3, 5). This difference in FC content may underlie the formation by fibroblasts of relatively more HDL particles containing two apoA-I molecules (peak III) compared with the situation in J774 cells (cf. Tables 1, 4). Whether or not any of these differences between human skin fibroblasts and mouse macrophages are attributable to differences in the properties of human and mouse ABCA1 remains to be determined. Although both fibroblasts and J774 macrophages secrete microparticles, the proportion of cellular lipid released into these particles compared with the nascent HDL is lower for fibroblasts. This difference between the two cell types may reflect a lower level of plasma membrane vesicle trafficking in fibroblasts compared with phagocytic macrophages.▪

REFERENCES

1. Yancey, P. G., A. E. Bortnick, G. Kellner-Weibel, M. de la Llera-Moya, M. C. Phillips, and G. H. Rothblat. 2003. Importance of different pathways of cellular cholesterol efflux. *Arterioscler. Thromb. Vasc. Biol.* **23:** 712–719.

2. Fielding, C. J., and P. E. Fielding. 1995. Molecular physiology of reverse cholesterol transport. *J. Lipid Res.* **36:** 211–228.

3. von Eckardstein, A., J. R. Nofer, and G. Assmann. 2001. High density lipoproteins and arteriosclerosis. Role of cholesterol efflux and reverse cholesterol transport. *Arterioscler. Thromb. Vasc. Biol.* **21:** 13–27.

4. Schultz, J. R., and E. M. Rubin. 1994. The properties of HDL in genetically engineered mice. *Curr. Opin. Lipidol.* **5:** 126–137.

5. Lee, J. Y., and J. S. Parks. 2005. ATP-binding cassette transporter AI and its role in HDL formation. *Curr. Opin. Lipidol.* **16:** 19–25.

6. Lewis, G. F., and D. J. Rader. 2005. New insights into the regulation of HDL metabolism and reverse cholesterol transport. *Circ. Res.* **96:** 1221–1232.

7. Barter, P. J. 2005. Cardioprotective effects of high-density lipoproteins: the evidence strengthens. *Arterioscler. Thromb. Vasc. Biol.* **25:** 1305–1306.

8. Yokoyama, S. 2000. Release of cellular cholesterol: molecular mechanism for cholesterol homeostasis in cells and in the body. *Biochim. Biophys. Acta.* **1529:** 231–244.

9. Brewer, H. B., Jr., A. T. Remaley, E. B. Neufeld, F. Basso, and C. Joyce. 2004. Regulation of plasma high-density lipoprotein levels by the ABCA1 transporter and the emerging role of high-density lipoprotein in the treatment of cardiovascular disease. *Arterioscler. Thromb. Vasc. Biol.* **24:** 1755–1760.

10. Oram, J. F. 2000. Tangier disease and ABCA1. *Biochim. Biophys. Acta.* **1529:** 321–330.

11. Lund-Katz, S., L. Liu, S. T. Thuahnai, and M. C. Phillips. 2003. High density lipoprotein structure. *Front. Biosci.* **8:** d1044–d1054.

12. Neufeld, E. B., A. T. Remaley, S. J. Demosky, J. A. Stonik, A. M. Cooney, M. Comly, N. K. Dwyer, M. Zhang, J. Blanchette-Mackie, S. Santamarina-Fojo, et al. 2001. Cellular localization and trafficking of the human ABCA1 transporter. *J. Biol. Chem.* **276:** 27584–27590.

13. Chen, W., Y. Sun, C. Welch, A. Gorelik, A. R. Leventhal, I. Tabas, and A. R. Tall. 2001. Preferential ATP-binding cassette transporter A1-mediated cholesterol efflux from late endosomes/lysosomes. *J. Biol. Chem.* **276:** 43564–43569.

14. Forte, T. M., J. K. Bielicki, R. Goth-Goldstein, J. Selmek, and M. R. McCall. 1995. Recruitment of cell phospholipids and cholesterol by apolipoproteins A-II and A-I: formation of nascent apolipoprotein-specific HDL that differ in size, phospholipid composition, and reactivity with LCAT. *J. Lipid Res.* **36:** 148–157.

15. Bielicki, J. K., M. R. McCall, and T. M. Forte. 1999. Apolipoprotein A-I promotes cholesterol release and apolipoprotein E recruitment from THP-1 macrophage-like foam cells. *J. Lipid Res.* **40:** 85–92.

16. Liu, L., A. E. Bortnick, M. Nickel, P. Dhanasekaran, P. V. Subbaiah, S. Lund-Katz, G. H. Rothblat, and M. C. Phillips. 2003. Effects of apolipoprotein A-I on ATP-binding cassette transporter A1-mediated efflux of macrophage phospholipid and cholesterol: formation of nascent high density lipoprotein particles. *J. Biol. Chem.* **278:** 42976–42984.

17. Hayashi, M., S. Abe-Dohmae, M. Okazaki, K. Ueda, and S. Yokoyama. 2005. Heterogeneity of high density lipoprotein generated by ABCA1 and ABCA7. *J. Lipid Res.* **46:** 1703–1711.

18. Krimbou, L., H. Hajj Hassan, S. Blain, S. Rashid, M. Denis, M. Marcil, and J. Genest. 2005. Biogenesis and speciation of nascent apoA-I-containing particles in various cell lines. *J. Lipid Res.* **46:** 1668–1677.

19. Lund-Katz, S., and M. C. Phillips. 1986. Packing of cholesterol molecules in human low-density lipoprotein. *Biochemistry.* **25:** 1562–1568.

20. Weisweiler, P. 1987. Isolation and quantitation of apolipoproteins A-I and A-II from human high-density lipoproteins by fast-protein liquid chromatography. *Clin. Chim. Acta.* **169:** 249–254.

21. Phillips, M. C., and K. E. Krebs. 1986. Studies of apolipoproteins at the air-water interface. *Methods Enzymol.* **128:** 387–403.

22. Krebs, K. E., J. A. Ibdah, and M. C. Phillips. 1988. A comparison of the surface activities of human apolipoproteins A-I and A-II at the air/water interface. *Biochim. Biophys. Acta.* **959:** 229–237.

23. Sakr, S. W., D. L. Williams, G. W. Stoudt, M. C. Phillips, and G. H. Rothblat. 1999. Induction of cellular cholesterol efflux to lipid-free apolipoprotein A-I by cAMP. *Biochim. Biophys. Acta.* **1438:** 85–98.

24. Bortnick, A. E., G. H. Rothblat, G. Stoudt, K. L. Hoppe, L. J. Royer, J. McNeish, and O. L. Francone. 2000. The correlation of ATP-binding cassette 1 mRNA levels with cholesterol efflux from various cell lines. *J. Biol. Chem.* **275:** 28634–28640.

25. Gillotte, K. L., M. Zaiou, S. Lund-Katz, G. M. Anantharamaiah, P. Holvoet, A. Dhoest, M. N. Palgunachari, J. P. Segrest, K. H. Weisgraber, G. H. Rothblat, et al. 1999. Apolipoprotein-mediated plasma membrane microsolubilization. Role of lipid affinity and

26. Favari, E., F. Bernini, P. Tarugi, G. Franceschini, and L. Calabresi. 2002. The C-terminal domain of apolipoprotein A-I is involved in ABCA1-driven phospholipid and cholesterol efflux. *Biochem. Biophys. Res. Commun.* **299:** 801–805.

27. Johnson, W. J., M. J. Bamberger, R. A. Latta, P. E. Rapp, M. C. Phillips, and G. H. Rothblat. 1986. The bidirectional flux of cholesterol between cells and lipoproteins. Effects of phospholipid depletion of high density lipoprotein. *J. Biol. Chem.* **261:** 5766–5776.

28. Rouser, G. 1973. Quantitative liquid column and thin layer chromatography of lipids and other water insoluble substances, elution selectivity principles, and a graphic method for pattern analysis of chromatographic data. *J. Chromatogr. Sci.* **11:** 60–76.

29. Bligh, E. G., and W. J. Dyer. 1959. A rapid method of total lipid extraction and purification. *Can. J. Biochem. Physiol.* **37:** 911–917.

30. Klansek, J. J., P. Yancey, R. W. St. Clair, R. T. Fischer, W. J. Johnson, and J. M. Glick. 1995. Cholesterol quantitation by GLC: artifactual formation of short-chain steryl esters. *J. Lipid Res.* **36:** 2261–2266.

31. Markwell, M. A., S. M. Haas, L. L. Bieber, and N. E. Tolbert. 1978. A modification of the Lowry procedure to simplify protein determination in membrane and lipoprotein samples. *Anal. Biochem.* **87:** 206–210.

32. Asztalos, B., W. Zhang, P. S. Roheim, and L. Wong. 1997. Role of free apolipoprotein A-I in cholesterol efflux. Formation of pre-alpha-migrating high-density lipoprotein particles. *Arterioscler. Thromb. Vasc. Biol.* **17:** 1630–1636.

33. Sparks, D. L., S. Lund-Katz, and M. C. Phillips. 1992. The charge and structural stability of apolipoprotein A-I in discoidal and spherical recombinant high density lipoprotein particles. *J. Biol. Chem.* **267:** 25839–25847.

34. Forte, T. M., and R. W. Nordhausen. 1986. Electron microscopy of negatively stained lipoproteins. *Methods Enzymol.* **128:** 442–457.

35. Yu, W., M. Ko, K. Yanagisawa, and M. Michikawa. 2005. Neurodegeneration in heterozygous Niemann-Pick type C1 (NPC1) mouse: implication of heterozygous NPC1 mutations being a risk for tauopathy. *J. Biol. Chem.* **280:** 27296–27302.

36. Satta, N., F. Toti, O. Feugeas, A. Bohbot, J. Dachary-Prigent, V. Eschwege, H. Hedman, and J. M. Freyssinet. 1994. Monocyte vesiculation is a possible mechanism for dissemination of membrane-associated procoagulant activities and adhesion molecules after stimulation by lipopolysaccharide. *J. Immunol.* **153:** 3245–3255.

37. Basso, F., L. Freeman, C. L. Knapper, A. Remaley, J. Stonik, E. B. Neufeld, T. Tansey, M. J. Amar, J. Fruchart-Najib, N. Duverger, et al. 2003. Role of the hepatic ABCA1 transporter in modulating intrahepatic cholesterol and plasma HDL cholesterol concentrations. *J. Lipid Res.* **44:** 296–302.

38. Timmins, J. M., J. Y. Lee, E. Boudyguina, K. D. Kluckman, L. R. Brunham, A. Mulya, A. K. Gebre, J. M. Coutinho, P. L. Colvin, T. L. Smith, et al. 2005. Targeted inactivation of hepatic Abca1 causes profound hypoalphalipoproteinemia and kidney hypercatabolism of apoA-I. *J. Clin. Invest.* **115:** 1333–1342.

39. Chroni, A., T. Liu, M. L. Fitzgerald, M. W. Freeman, and V. I. Zannis. 2004. Cross-linking and lipid efflux properties of apoA-I mutants suggest direct association between apoA-I helices and ABCA1. *Biochemistry.* **43:** 2126–2139.

40. Vedhachalam, C., L. Liu, M. Nickel, P. Dhanasekaran, G. M. Anantharamaiah, S. Lund-Katz, G. H. Rothblat, and M. C. Phillips. 2004. Influence of apoA-I structure on the ABCA1-mediated efflux of cellular lipids. *J. Biol. Chem.* **279:** 49931–49939.

41. Denis, M., B. Haidar, M. Marcil, M. Bouvier, L. Krimbou, and J. Genest, Jr. 2004. Molecular and cellular physiology of apolipoprotein A-I lipidation by the ATP-binding cassette transporter A1 (ABCA1). *J. Biol. Chem.* **279:** 7384–7394.

42. Davidson, W. S., D. L. Sparks, S. Lund-Katz, and M. C. Phillips. 1994. The molecular basis for the difference in charge between pre-beta- and alpha-migrating high density lipoproteins. *J. Biol. Chem.* **269:** 8959–8965.

43. Zhang, W., B. Asztalos, P. S. Roheim, and L. Wong. 1998. Characterization of phospholipids in pre-alpha HDL: selective phospholipid efflux with apolipoprotein A-I. *J. Lipid Res.* **39:** 1601–1607.

44. Gillotte-Taylor, K., M. Nickel, W. J. Johnson, O. L. Francone, P. Holvoet, S. Lund-Katz, G. H. Rothblat, and M. C. Phillips. 2002. Effects of enrichment of fibroblasts with unesterified cholesterol on the efflux of cellular lipids to apolipoprotein A-I. *J. Biol. Chem.* **277:** 11811–11820.

45. Davidson, W. S., and R. A. Silva. 2005. Apolipoprotein structural

membrane penetration in the efflux of cellular cholesterol and phospholipid. *J. Biol. Chem.* **274:** 2021–2028.

organization in high density lipoproteins: belts, bundles, hinges and hairpins. *Curr. Opin. Lipidol.* **16:** 295–300.

46. Haberland, M. E., and J. A. Reynolds. 1975. Interaction of L-alpha-palmitoyl lysophosphatidylcholine with the AI polypeptide of high density lipoprotein. *J. Biol. Chem.* **250:** 6636–6639.

47. Pike, L. J. 2003. Lipid rafts: bringing order to chaos. *J. Lipid Res.* **44:** 655–667.

48. Alder-Baerens, N., P. Muller, A. Pohl, T. Korte, Y. Hamon, G. Chimini, T. Pomorski, and A. Herrmann. 2005. Headgroup-specific exposure of phospholipids in ABCA1-expressing cells. *J. Biol. Chem.* **280:** 26321–26329.

49. Smith, J. D., C. Waelde, A. Horwitz, and P. Zheng. 2002. Evaluation of the role of phosphatidylserine translocase activity in ABCA1-mediated lipid efflux. *J. Biol. Chem.* **277:** 17797–17803.

50. Chen, W., N. Wang, and A. R. Tall. 2005. A PEST deletion mutant of ABCA1 shows impaired internalization and defective cholesterol efflux from late endosomes. *J. Biol. Chem.* **280:** 29277–29281.

51. Yamauchi, Y., C. C. Chang, M. Hayashi, S. Abe-Dohmae, P. C. Reid, T. Y. Chang, and S. Yokoyama. 2004. Intracellular cholesterol mobilization involved in the ABCA1/apolipoprotein-mediated assembly of high density lipoprotein in fibroblasts. *J. Lipid Res.* **45:** 1943–1951.

52. Neufeld, E. B., J. A. Stonik, S. J. Demosky, Jr., C. L. Knapper, C. A. Combs, A. Cooney, M. Comly, N. Dwyer, J. Blanchette-Mackie, A. T. Remaley, et al. 2004. The ABCA1 transporter modulates late endocytic trafficking: insights from the correction of the genetic defect in Tangier disease. *J. Biol. Chem.* **279:** 15571–15578.

53. Takahashi, Y., and J. D. Smith. 1999. Cholesterol efflux to apolipo-protein AI involves endocytosis and resecretion in a calcium-dependent pathway. *Proc. Natl. Acad. Sci. USA.* **96:** 11358–11363.

54. Hao, M., S. Mukherjee, Y. Sun, and F. R. Maxfield. 2004. Effects of cholesterol depletion and increased lipid unsaturation on the properties of endocytic membranes. *J. Biol. Chem.* **279:** 14171–14178.

55. Hugel, B., M. C. Martinez, C. Kunzelmann, and J. M. Freyssinet. 2005. Membrane microparticles: two sides of the coin. *Physiology (Bethesda).* **20:** 22–27.

56. Freyssinet, J. M. 2003. Cellular microparticles: what are they bad or good for? *J. Thromb. Haemost.* **1:** 1655–1662.

57. Parton, R. G. 1994. Ultrastructural localization of gangliosides: GM1 is concentrated in caveolae. *J. Histochem. Cytochem.* **42:** 155–166.

58. Mallat, Z., B. Hugel, J. Ohan, G. Leseche, J. M. Freyssinet, and A. Tedgui. 1999. Shed membrane microparticles with procoagulant potential in human atherosclerotic plaques: a role for apoptosis in plaque thrombogenicity. *Circulation.* **99:** 348–353.

59. Oram, J. F. 2002. ATP-binding cassette transporter A1 and cholesterol trafficking. *Curr. Opin. Lipidol.* **13:** 373–381.

60. Nguyen, D. G., A. Booth, S. J. Gould, and J. E. Hildreth. 2003. Evidence that HIV budding in primary macrophages occurs through the exosome release pathway. *J. Biol. Chem.* **278:** 52347–52354.

61. Combes, V., N. Coltel, M. Alibert, M. van Eck, C. Raymond, I. Juhan-Vague, G. E. Grau, and G. Chimini. 2005. ABCA1 gene deletion protects against cerebral malaria: potential pathogenic role of microparticles in neuropathology. *Am. J. Pathol.* **166:** 295–302.

ABCA1-mediated cholesterol efflux   843